The coupled mode parabolic equation

Ahmad T. Abawi[a] and W. A. Kuperman
Scripps Institution of Oceanography, La Jolla, California 92093

Michael D. Collins
Naval Research Laboratory, Washington, DC 20375

(Received 3 September 1996; accepted for publication 4 February 1997)

The coupled mode parabolic equation (PE) is a generalization of the adiabatic mode PE that includes mode coupling terms. It is practical to apply this approach to large-scale problems involving coupling of energy between both modes and azimuths. The solution is expressed in terms of the normal modes and mode coefficients, which satisfy coupled horizontal wave equations. The coupled mode PE may be solved efficiently with the splitting method. The first step is equivalent to solving the adiabatic mode PE over one range step. The second step involves the integration of the coupling term. The coupling mode PE solution conserves energy, which is an important aspect of a range-dependent propagation model. The derivation of the coupled mode PE, which involves completing the square of an operator, is related to the derivation of an adiabatic mode PE that accounts for ambient flow. Examples are presented to illustrate the accuracy of the coupled mode PE. © *1997 Acoustical Society of America.* [S0001-4966(97)05406-4]

PACS numbers: 43.30.Bp, 43.30.Dr [SAC-B]

INTRODUCTION

The Perth–Bermuda[1–3] and Heard Island[4–7] experiments have stimulated interest in global-scale ocean acoustics. It is very difficult to solve global-scale problems due to the size and complexity of the medium and the coupling of energy between both modes and azimuths. The global-scale results that have been generated[2,3,5–8] neglect one type of coupling and are based on adiabatic mode,[9–12] parabolic equation (PE),[13–16] and ray approximations. There are indications that both types of coupling occur for some global-scale problems.[5] Three-dimensional PE models[17,18] handle both types of coupling but are only practical for small-scale problems. In this paper, we derive and test a generalization of the adiabatic mode PE[19] that includes coupling terms. It is practical to apply the coupled mode PE to large-scale problems and possibly even global-scale problems at low frequencies.

The adiabatic mode solution is based on the assumption that energy does not couple between the modes (or eigenfunctions) of the depth separated wave equation. The acoustic field is represented locally in terms of the modes, and the mode coefficients satisfy horizontal wave equations. In some cases, it is possible to obtain useful information by solving for only a fraction of the mode coefficients. The horizontal wave equations may be solved efficiently with the PE method,[19] which handles caustics and horizontal variations in the properties of the medium. At low frequencies, it is practical to solve global-scale problems with the adiabatic mode PE.[8] This approach is more efficient than three-dimensional PE models because the number of propagating modes is usually much smaller than the number of grid points that are required in a finite-difference treatment of the depth operator.

The coupled mode PE is obtained by including coupling terms[20–29] in the horizontal wave equations. Mode coupling may also be treated using vertical interface conditions.[30] The splitting solution[31] of the coupled mode PE involves the numerical solution of the adiabatic mode PE (which does not involve coupled equations) and the integration of a mode coupling term (which does not involve azimuthal coupling). The coupled mode PE solution conserves energy, which is an important property of a range-dependent propagation model.[32–34] The derivation of the coupled mode PE involves completing the square of an operator and is similar to the derivation of the windy PE,[35] which is a generalization of the adiabatic mode PE that accounts for ambient flow. The derivation of the coupled mode PE is presented in Sec. I. Examples are presented in Sec. II to illustrate the accuracy of the coupled mode PE.

I. DERIVATION

We derive the coupled mode PE in this section. To simplify the derivation, we work in Cartesian coordinates and neglect attenuation. We later convert to cylindrical coordinates and include the effects of attenuation as a perturbation by allowing the modal eigenvalues to be complex.[30] The sound speed c and density ρ may vary arbitrarily with the depth z but are assumed to vary gradually with the range x and cross range y. We place a time-harmonic point source of circular frequency ω on the z axis and remove the factor $\exp(-i\omega t)$ from the complex pressure P.

In order to handle density variations efficiently we work with the reduced pressure $p = \rho^{-1/2}P$, which satisfies the Helmholtz equation,

$$\nabla_\perp^2 p + \frac{\partial^2 p}{\partial z^2} + \tilde{k}^2 p = 0, \tag{1}$$

[a]Present address: Naval Command Control, Ocean Survey Center, San Diego, CA 92152.

$$\widetilde{k}^2 = k^2 + \frac{1}{2}\frac{\partial^2 \gamma}{\partial z^2} - \frac{1}{4}\left(\frac{\partial \gamma}{\partial z}\right)^2, \tag{2}$$

where $k=\omega/c$ is the wave number, $\gamma=\log \rho$, and $\nabla_\perp^2$ is the horizontal component of the Laplacian. The solution of Eq. (1) is expressed in terms of the local normal modes as

$$p(x,y,z) = \sum_j p_j(x,y)\phi_j(z;x,y), \tag{3}$$

where p_j is the jth mode coefficient and the jth mode ϕ_j and eigenvalue $k_j^2(x,y)$ satisfy

$$\frac{\partial^2 \phi_j}{\partial z^2} + \widetilde{k}^2 \phi_j = k_j^2 \phi_j, \tag{4}$$

$$\int \phi_i \phi_j \, dz = \delta_{ij}. \tag{5}$$

The semicolon in the argument of ϕ_j indicates slow variation with respect to the horizontal coordinates. To obtain a leading-order mode coupling correction in the limit of gradual horizontal variations in c and ρ, we retain only the first horizontal derivatives of ϕ_j. We later account for horizontal variations in k_j by including an energy-conservation correction.

Substituting the normal mode representation into Eq. (1), we obtain

$$\sum_j \phi_j(\nabla_\perp^2 p_j + k_j^2 p_j) \sim -2\sum_j \left(\frac{\partial \phi_j}{\partial x}\frac{\partial p_j}{\partial x} + \frac{\partial \phi_j}{\partial y}\frac{\partial p_j}{\partial y}\right). \tag{6}$$

Multiplying Eq. (6) by ϕ_i, integrating over depth, and using Eq. (5), we obtain the horizontal wave equations,

$$\nabla_\perp^2 p_i + k_i^2 p_i \sim -2\sum_j \left(A_{x,i,j}\frac{\partial p_j}{\partial x} + A_{y,i,j}\frac{\partial p_j}{\partial y}\right), \tag{7}$$

where the coupling coefficients $A_{x,i,j}$ and $A_{y,i,j}$ are defined by

$$A_{x,i,j} = \int \phi_i \frac{\partial \phi_j}{\partial x}\, dz, \tag{8}$$

$$A_{y,i,j} = \int \phi_i \frac{\partial \phi_j}{\partial y}\, dz. \tag{9}$$

The adiabatic mode solution is recovered by neglecting the terms on the right side of Eq. (7). Placing the mode coefficients into the vector **p**, the coupling coefficients into the matrices A_x and A_y, and the eigenvalues into the diagonal matrix K^2, we obtain

$$\frac{\partial^2 \mathbf{p}}{\partial x^2} + \frac{\partial^2 \mathbf{p}}{\partial y^2} + K^2\mathbf{p} + 2A_x\frac{\partial \mathbf{p}}{\partial x} + 2A_y\frac{\partial \mathbf{p}}{\partial y} = \mathbf{0}. \tag{10}$$

It follows from Eq. (5) that the coupling matrices $A_x = -A_x^t$ and $A_y = -A_y^t$ are antisymmetric. We refer to solutions of Eq. (10) as continuous coupled mode solutions as opposed to the stepwise coupled mode solutions of Ref. 30.

Completing the square of the range operator in Eq. (10) and neglecting a higher-order coupling term, we obtain

$$\left(\frac{\partial}{\partial x} + A_x\right)^2 \mathbf{p} + \frac{\partial^2 \mathbf{p}}{\partial y^2} + 2A_y\frac{\partial \mathbf{p}}{\partial y} + K^2\mathbf{p} = \mathbf{0}. \tag{11}$$

Factoring the operator in Eq. (11) under the assumption of gradual range dependence, we obtain

$$\left[\frac{\partial}{\partial x} + A_x - i\left(\frac{\partial^2}{\partial y^2} + 2A_y\frac{\partial}{\partial y} + K^2\right)^{1/2}\right] \times \left[\frac{\partial}{\partial x} + A_x + i\left(\frac{\partial^2}{\partial y^2} + 2A_y\frac{\partial}{\partial y} + K^2\right)^{1/2}\right]\mathbf{p} = \mathbf{0}. \tag{12}$$

This approach for factoring Eq. (10) was used to derive the windy PE from a similar horizontal wave equation in which advection terms play the role of the coupling terms.[35] Assuming that outgoing energy dominates backscattered energy, we obtain the outgoing wave equation:

$$\frac{\partial \mathbf{p}}{\partial x} = -A_x\mathbf{p} + i\left(\frac{\partial^2}{\partial y^2} + 2A_y\frac{\partial}{\partial y} + K^2\right)^{1/2}\mathbf{p}. \tag{13}$$

In cylindrical geometry, we remove the spreading factor $r^{-1/2}$ from **p** and obtain the following counterpart to Eq. (13):

$$\frac{\partial \mathbf{p}}{\partial r} = -A_r\mathbf{p} + i\left(\frac{1}{r^2}\frac{\partial^2}{\partial \theta^2} + 2A_\theta\frac{1}{r}\frac{\partial}{\partial \theta} + K^2\right)^{1/2}\mathbf{p}, \tag{14}$$

where the entries of A_r and A_θ are defined by

$$A_{r,i,j} = \int \phi_i \frac{\partial \phi_j}{\partial r}\, dz, \tag{15}$$

$$A_{\theta,i,j} = \int \phi_i \frac{1}{r}\frac{\partial \phi_j}{\partial \theta}\, dz. \tag{16}$$

When acoustic energy propagates from a point source in a medium with gradual horizontal variations, azimuthal terms are usually dominated by other terms in the wave equation. For many problems, it is possible to ignore azimuthal terms altogether and apply the uncoupled azimuth approximation.[36] Even when azimuthal coupling is significant, the azimuthal terms tend to be less important than other terms (e.g., the three-dimensional PE models of Refs. 17 and 18 are based on a narrow-angle expansion in the azimuth term but a wide-angle expansion in the depth term). We use this fact and observations of solutions of the windy PE to motivate a useful simplification of Eq. (14). The windy PE is based on the following outgoing wave equation that is similar to Eq. (14):

$$\frac{\partial p_j}{\partial r} = -ik_jU_{jr}p_j + i\left(\frac{1}{r^2}\frac{\partial^2}{\partial \theta^2} + 2ik_jU_{j\theta}\frac{1}{r}\frac{\partial}{\partial \theta} + k_j^2\right)^{1/2} p_j, \tag{17}$$

where U_{jr} and $U_{j\theta}$ are defined in terms of the wind velocity.[35] We have found that the cross term in Eq. (17), which involves the product of a flow operator and an azimuthal coupling operator, tends to be dominated by the other terms. In particular, the solutions of the equation

$$\frac{\partial p_j}{\partial r} = -ik_jU_{jr}p_j + i\left(\frac{1}{r^2}\frac{\partial^2}{\partial \theta^2} + k_j^2\right)^{1/2} p_j \tag{18}$$

are nearly identical to the solutions of Eq. (17) for the examples presented in Ref. 35.

Neglecting the cross term in Eq. (14), we obtain the coupled mode PE,

$$\frac{\partial \mathbf{p}}{\partial r} = -A_r \mathbf{p} + i\left(\frac{1}{r^2}\frac{\partial^2}{\partial \theta^2} + K^2\right)^{1/2} \mathbf{p}. \tag{19}$$

The first term on the right side of Eq. (19) accounts for mode coupling in the radial direction. The second term accounts for azimuthal coupling and refraction. Neglecting the cross term to obtain Eq. (18) does not provide a significant advantage for the windy PE. Neglecting the cross term to obtain Eq. (19) leads to a significant simplification of the numerical solution of the coupled mode PE because it permits the use of alternating directions. Neglecting the cross term can be justified by an asymptotic argument. We regard azimuthal coupling as a perturbation and retain only the leading order mode coupling correction to the adiabatic mode PE. Since $A_r\mathbf{p}$ and $A_\theta \mathbf{p}$ are of the same order, it follows that

$$\left| K^{-1} A_\theta \frac{1}{r} \frac{\partial \mathbf{p}}{\partial \theta} \right| \ll |A_r \mathbf{p}|. \tag{20}$$

In other words, the first term on the right side of Eq. (14) dominates the cross term.

The solution of Eq. (19) does not conserve energy. One approach for deriving a coupled mode PE that conserves energy would be to perform a WKB analysis that includes horizontal derivatives of the environmental parameters. An easier approach is to incorporate previous results and then verify that energy is conserved. Energy-conserving solutions can be obtained by defining a new dependent variable that is related to the energy-flux density. The dependent variable in Eq. (19) is missing the correction factor $k_j^{1/2}$ that occurs in the complete energy conservation correction.[34] Applying this correction as described in Ref. 19, we define $u_j = k_j^{1/2} p_j$ and obtain the energy-conserving coupled mode PE solution,

$$p(r,\theta,z) = r^{-1/2} \sum_j [k_j(r,\theta)]^{-1/2} u_j(r,\theta) \phi_j(z;r,\theta), \tag{21}$$

$$\frac{\partial \mathbf{u}}{\partial r} = -A_r \mathbf{u} + i\left(\frac{1}{r^2}\frac{\partial^2}{\partial \theta^2} + K^2\right)^{1/2} \mathbf{u}, \tag{22}$$

where u_j is the jth entry of $\mathbf{u}$. The initial condition corresponding to a point source at $z = z_0$ is

$$u_j(0,\theta) = \phi_j(z_0;0,\theta). \tag{23}$$

The second term on the right side of Eq. (22) conserves energy because the adiabatic mode PE conserves energy.[19] The coupling term produces a rotation of $\mathbf{u}$ and conserves energy because

$$\frac{dE}{dr} = \mathbf{u}^* \frac{\partial \mathbf{u}}{\partial r} + \frac{\partial \mathbf{u}^*}{\partial r} \mathbf{u} = -\mathbf{u}^* A_r \mathbf{u} - \mathbf{u}^* A_r^t \mathbf{u} = 0, \tag{24}$$

where $E = |\mathbf{u}|^2$ is the energy flux. The third equal sign in Eq. (24) follows from the antisymmetry of A_r.

We solve Eq. (22) with the splitting method,[31] which involves numerical solutions of the equations

$$\frac{\partial \mathbf{u}}{\partial r} = i\left(\frac{1}{r^2}\frac{\partial^2}{\partial \theta^2} + K^2\right)^{1/2} \mathbf{u}, \tag{25}$$

$$\frac{\partial \mathbf{u}}{\partial r} = -A_r \mathbf{u}. \tag{26}$$

Since K^2 is diagonal and the cross term in Eq. (14) was dropped, Eq. (25) is an uncoupled system that reduces to the horizontal wave equations involved in the adiabatic mode PE solution. We therefore solve Eq. (25) over a range step using the approach described in Ref. 19. The operator square root is approximated using a rational function expansion about the representative horizontal wave number k_0. Crank–Nicolson integration is used for the range discretization. The azimuth discretization involves a tridiagonal matrix modified with entries in the upper right and lower left corners to account for periodicity. The numerical solution of Eq. (26) is obtained using Crank–Nicolson integration.

There are several possible ways to extend or improve the coupled mode PE. When coupling is mostly into neighboring modes, it is possible to improve efficiency by approximating A_r with a banded matrix.[12] The coupled mode PE can be modified to account for energy loss due to coupling into the nonpropagating or nontrapped modes by including positive entries along the main diagonal of the coupling matrix. It should be possible to include the effects of coupling with the stepwise approach of Ref. 30 as an alternative to using the coupling term in Eq. (19). With this approach, the medium is approximated by a sequence of range-independent regions and the transmitted fields across vertical interfaces are approximated with the energy-conserving condition described in Ref. 34. This approach includes higher-order coupling terms and is a generalization of the step-wise coupled mode solution to three dimensions.

II. IMPLEMENTATION AND EXAMPLES

In this section, we present examples to illustrate and test solutions of the coupled mode PE. Although several papers have been published on continuous coupled modes, there apparently has not been any benchmark testing to confirm that this technique actually works. The implementation of the coupled mode PE involves the solution of the eigenvalue problem throughout the region of interest. Once the eigenvalues, eigenfunctions, and coupling coefficients are obtained and stored, the coupled mode PE solution may be obtained efficiently for different combinations of source and receiver locations. For the adiabatic case, this precalculation approach[12] has been used to solve problems in matched-field processing[37,38] that require replica fields for large numbers of source and receiver locations[39]

Example A is a two-dimensional problem involving a 25-Hz source at $z = 50$ m in a 200-m-thick waveguide that is lossless and of constant density. The waveguide consists of two layers that are divided by an interface at

$$z = \begin{cases} d_0 & \text{for } r < 1 \text{ km} \\ d_0 + \alpha \sin\left(\dfrac{2\pi r}{\lambda}\right) & \text{for } r > 1 \text{ km}, \end{cases} \tag{27}$$

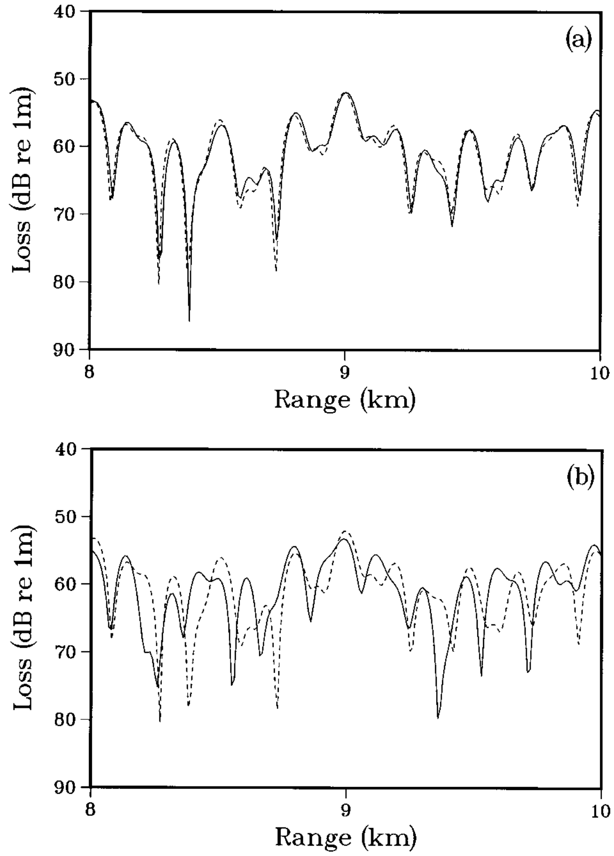

FIG. 1. Transmission loss at $z=30$ m for example A, which is a two-dimensional problem that involves a sinusoidal interface between two homogeneous layers. The solid curves correspond to (a) the coupled mode PE solution and (b) the adiabatic mode solution. The dashed curves correspond to the energy-conserving PE solution.

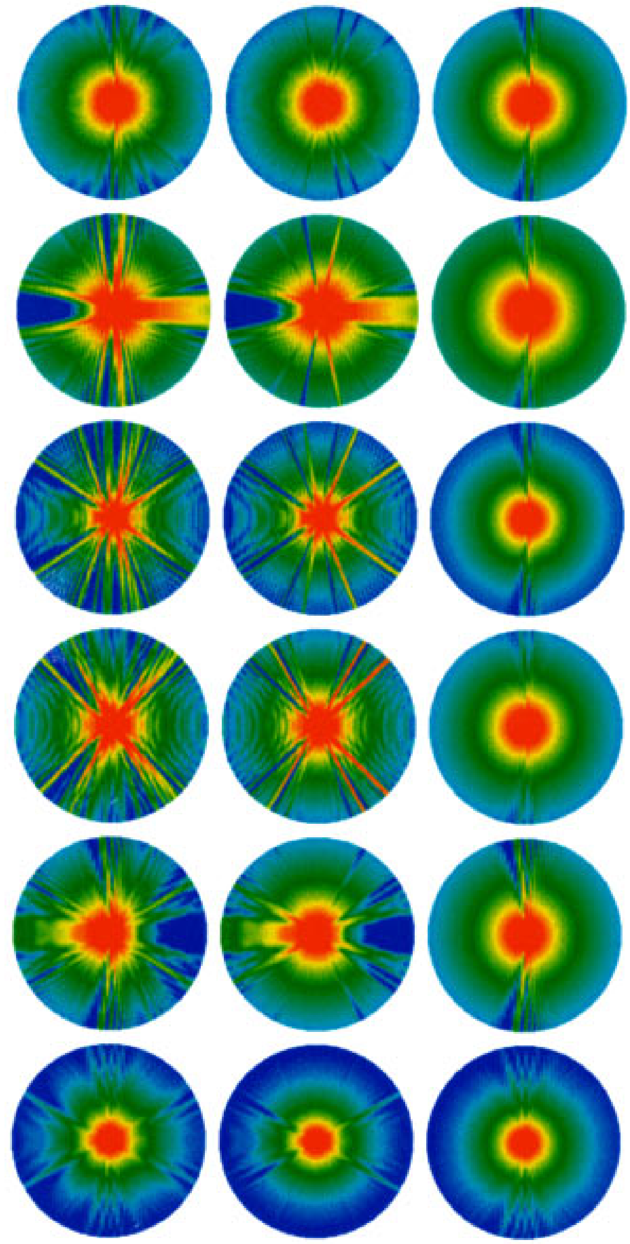

FIG. 2. The mode coefficients for example B, which is a three-dimensional problem that involves a corrugated interface between two homogeneous layers. The maximum range is 5 km, the positive x direction is to the right, and the positive y direction is to the top. The left column contains the coupled mode PE solutions, the center column contains the uncoupled azimuth solution, and the right column contains the adiabatic mode PE solution. The modes are shown in increasing order going downward in each column. The dynamic range is 10 dB, with red corresponding to the highest intensities.

where $d_0=100$ m, $\alpha=5$ m, and $\lambda=200$ m. The speed of sound is 1500 m/s in the upper layer and 1600 m/s in the lower layer. The purpose of this example is to show that the coupling term accurately handles extensive mode coupling. The waveguide supports six modes corresponding to horizontal phase speeds that range between about 1538 and 4190 m/s. Results for example A appear in Fig. 1. The coupled mode PE solution is in agreement with a reference solution that was generated using a finite-difference PE model based on the complete energy-conservation correction.[34] The adiabatic mode solution breaks down for this problem.

Example B is identical to example A, with the exception that the interface is at

$$z=d_0+\alpha \sin\left(\frac{2\pi x}{\lambda}\right). \tag{28}$$

We were motivated to consider this problem because corrugated interfaces can cause azimuthal coupling by channeling energy in the y direction.[17] To handle the wide range of horizontal phase speeds, we take $\omega/k_0=2000$ m/s and approximate the operator square root in Eq. (22) with an eight-term rational function. We use range and azimuthal grid spacings of 10 m and 0.25°. Results for example B appear in Fig. 2. Since both types of coupling are important for this problem, there are significant differences between the coupled mode PE solution and the solutions that neglect one type of coupling. Comparing the left and center columns, we observe that azimuthal coupling is strongest near the y axis, where the corrugations cause channeling. Comparing the left and right columns, we observe that mode coupling is strongest near the x axis, where range dependence is greatest.

Example C involves a 25-Hz source at $z=180$ m in a shallow water ocean environment. The sound speed is 1500 m/s in the water column and 1700 m/s in the sediment. The density of the sediment is 1.5 times the density of the water. The attenuation in the sediment is 0.5 dB/λ. The ocean depth

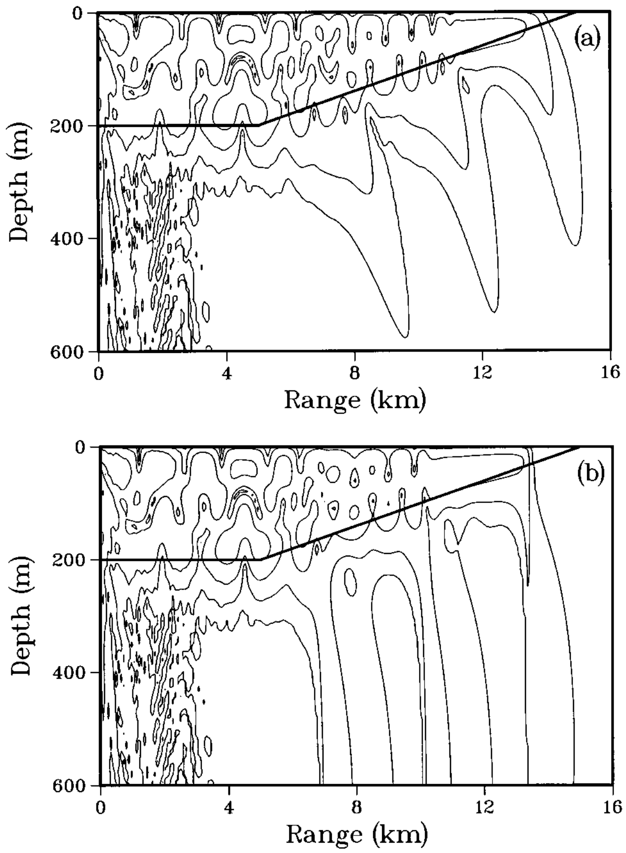

FIG. 3. Transmission loss contours for example C, which involves a sloping ocean bottom and mode cutoff. (a) The coupled mode PE solution. (b) The adiabatic mode solution.

is 200 m for $r<5$ km and linearly decreases to an apex at $r=15$ km. In the upslope region, the three trapped modes cut off and couple into beams in the sediment.[40] The purpose of this example is to illustrate the coupled mode PE for a realistic example and to illustrate coupling between trapped and nontrapped modes. We truncate the domain at $z=1200$ m and use 36 modes in the coupled mode PE calculation. Contour plots for example C appear in Fig. 3. The adiabatic mode solution breaks down in the sediment (the beams are not correct). The coupled mode PE solution is accurate in the sediment (the beams are correct).

III. CONCLUSION

The coupled mode PE was derived by including a coupling term in the adiabatic mode PE. This technique is efficient for solving acoustic propagation problems that involve both mode and azimuthal coupling. The coupled mode PE is simplified by neglecting a higher-order cross term that involves a product of mode and azimuthal coupling operators. Tests involving a similar cross term in the windy PE suggest that this approximation is robust. The numerical solution is based on standard techniques such as splitting and Crank–Nicolson integration. The coupled mode PE conserves energy because the adiabatic mode PE conserves energy and the coupling matrix is antisymmetric. The accuracy of the coupled mode PE was demonstrated for benchmark problems. The coupled mode PE was also applied to solve a three-dimensional problem.

ACKNOWLEDGMENTS

This work was supported by the Office of Naval Research, Code 321OA, and DARPA Grant No. MDA972-93-1-0003.

[1] R. C. Shockley, J. Northrop, P. G. Hansen, and C. Hartdegen, ''SOFAR propagation paths from Australia to Bermuda: Comparison of signal speed algorithms and experiments,'' J. Acoust. Soc. Am. **71**, 51–60 (1982).

[2] W. C. O'Reilly, W. H. Munk, and J. L. Reid, ''Australia–Bermuda sound transmission experiment (1960) revised,'' J. Phys. Oceanogr. **18**, 1878–1898 (1988).

[3] K. D. Heaney, W. A. Kuperman, and B. E. McDonald, ''Perth–Bermuda sound propagation (1960): Adiabatic mode interpretation,'' J. Acoust. Soc. Am. **90**, 2586–2594 (1991).

[4] W. H. Munk, R. C. Spindel, A. Baggeroer, and T. G. Birdsall, ''The Heard Island feasibility test,'' J. Acoust. Soc. Am. **96**, 2330–2342 (1994).

[5] B. E. McDonald, M. D. Collins, W. A. Kuperman, and K. D. Heaney, ''Comparison of data and model predictions for Heard Island acoustic transmissions,'' J. Acoust. Soc. Am. **96**, 2357–2370 (1994).

[6] E. C. Shang, Y. Y. Wang, and T. M. Georges, ''Dispersion and repopulation of the Heard–Ascension modes,'' J. Acoust. Soc. Am. **96**, 2371–2379 (1994).

[7] C. S. Chiu, A. J. Semtner, C. M. Ort, J. H. Miller, and L. L. Ehret, ''A ray variability analysis of sound transmission from Heard Island to California,'' J. Acoust. Soc. Am. **96**, 2380–2388 (1994).

[8] M. D. Collins, B. E. McDonald, K. D. Heaney, and W. A. Kuperman, ''Three-dimensional effects in global acoustics,'' J. Acoust. Soc. Am. **97**, 1567–1575 (1995).

[9] A. D. Pierce, ''Extension of the method of normal modes to sound propagation in an almost-stratified medium,'' J. Acoust. Soc. Am. **37**, 19–27 (1965).

[10] D. M. Milder, ''Ray and wave invariants for SOFAR channel propagation,'' J. Acoust. Soc. Am. **46**, 1259–1263 (1969).

[11] H. Weinberg and R. Burridge, ''Horizontal ray theory for ocean acoustics,'' J. Acoust. Soc. Am. **55**, 63–79 (1974).

[12] W. A. Kuperman, M. B. Porter, J. S. Perkins, and R. B. Evans, ''Rapid computation of acoustic fields in three-dimensional ocean environments,'' J. Acoust. Soc. Am. **89**, 125–133 (1991).

[13] M. A. Leontovich and V. A. Fock, ''Solution of the problem of propagation of electromagnetic waves along the earth's surface by the method of parabolic equation,'' J. Exp. Theor. Phys. **16**, 557–573 (1946).

[14] V. A. Fock, *Electromagnetic Diffraction and Propagation Problems* (Pergamon, New York, 1965), pp. 213–234.

[15] F. D. Tappert, ''The parabolic approximation method,'' in *Wave Propagation and Underwater Acoustics*, edited by J. B. Keller and J. S. Papadakis, Lecture Notes in Physics 70 (Springer-Verlag, New York, 1977).

[16] F. B. Jensen, W. A. Kuperman, M. B. Porter, and H. Schmidt, *Computational Ocean Acoustics* (American Institute of Physics, New York, 1994), pp. 343–412.

[17] M. D. Collins and S. A. Chin-Bing, ''A three-dimensional parabolic equation model that includes the effects of rough boundaries,'' J. Acoust. Soc. Am. **87**, 1104–1109 (1990).

[18] D. Lee, G. Botseas, and W. L. Siegmann, ''Examination of three-dimensional effects using a propagation model with azimuth-coupling capability (FOR3D),'' J. Acoust. Soc. Am. **91**, 3192–3202 (1992).

[19] M. D. Collins, ''The adiabatic mode parabolic equation,'' J. Acoust. Soc. Am. **94**, 2269–2278 (1993).

[20] R. D. Graves, A. Nagl, H. Überall, and G. L. Zarur, ''Range-dependent normal modes in underwater sound propagation: Application to the wedge-shaped ocean,'' J. Acoust. Soc. Am. **58**, 1171–1177 (1975).

[21] S. R. Rutherford, ''An examination of coupled mode theory as applied to underwater sound propagation,'' Rep. No. APL-TR-79-44 (Applied Research Laboratories, Austin, TX, 1979).

[22] S. R. Rutherford and K. E. Hawker, ''Consistent coupled mode theory of sound propagation for a class of nonseparable problems,'' J. Acoust. Soc. Am. **70**, 554–564 (1981).

[23] S. T. McDaniel, ''Mode coupling due to interaction with the seabed,'' J. Acoust. Soc. Am. **72**, 916–923 (1982).
[24] C. A. Boyles, ''Coupled mode solution for a cylindrically symmetric oceanic waveguide with a range and depth dependent refractive index and a time varying rough sea surface,'' J. Acoust. Soc. Am. **73**, 800–805 (1983).
[25] J. A. Fawcett, ''A derivation of the differential equations of coupled-mode propagation,'' J. Acoust. Soc. Am. **92**, 290–295 (1992).
[26] G. Gillette, ''Coupled modes in a waveguide with a range-dependent rigid basement,'' J. Acoust. Soc. Am. **95**, 187–200 (1994).
[27] D. P. Knobles, ''Solutions of coupled-mode equations with a large dimension in underwater acoustics,'' J. Acoust. Soc. Am. **96**, 1741–1747 (1994).
[28] Y. Desaubies and K. Dysthe, ''Normal-mode propagation in slowly varying ocean waveguides,'' J. Acoust. Soc. Am. **97**, 933–946 (1995).
[29] B. E. McDonald, ''Bathymetric and volumetric contributions in ocean acoustic mode coupling,'' J. Acoust. Soc. Am. **100**, 219–224 (1996).
[30] R. B. Evans, ''A coupled mode solution for acoustic propagation in a waveguide with stepwise depth variations of a penetrable bottom,'' J. Acoust. Soc. Am. **74**, 188–195 (1983).
[31] A. R. Mitchell and D. F. Griffiths, *The Finite Difference Method in Partial Differential Equations* (Wiley, New York, 1980), pp. 59–70.
[32] M. B. Porter, F. B. Jensen, and C. M. Ferla, ''The problem of energy conservation in one-way models,'' J. Acoust. Soc. Am. **89**, 1058–1067 (1991).
[33] M. D. Collins and E. K. Westwood, ''A higher-order energy-conserving parabolic equation for range-dependent ocean depth, sound speed, and density,'' J. Acoust. Soc. Am. **89**, 1068–1075 (1991).
[34] M. D. Collins, ''An energy-conserving parabolic equation for elastic media,'' J. Acoust. Soc. Am. **94**, 975–982 (1993).
[35] M. D. Collins, B. E. McDonald, W. A. Kuperman, and W. L. Siegmann, ''Jovian acoustics and Comet Shoemaker–Levy 9,'' J. Acoust. Soc. Am. **97**, 2147–2158 (1995).
[36] J. S. Perkins and R. N. Baer, ''An approximation to the three-dimensional parabolic-equation method for acoustic propagation,'' J. Acoust. Soc. Am. **72**, 515–522 (1982).
[37] H. P. Bucker, ''Use of calculated sound fields and matched-field detection to locate sound sources in shallow water,'' J. Acoust. Soc. Am. **59**, 368–373 (1976).
[38] A. B. Baggeroer, W. A. Kuperman, and P. N. Mikhalevsky, ''An overview of matched field methods in ocean acoustics,'' IEEE J. Ocean Eng. **18**, 401–424 (1993).
[39] J. S. Perkins and W. A. Kuperman, ''Environmental signal processing: Three-dimensional matched-field processing with a vertical array,'' J. Acoust. Soc. Am. **87**, 1553–1556 (1990).
[40] F. B. Jensen and W. A. Kuperman, ''Sound propagation in a wedge-shaped ocean with a penetrable bottom,'' J. Acoust. Soc. Am. **67**, 1564–1566 (1980).